

A STAGE CALCULATION IN A CENTRIFUGAL COMPRESSOR

C.V. Wallis

Z.M. Moussa

B.N. Srivastava

GE Aircraft Engines, Lynn, MA 01910

ABSTRACT

The results of an analytical study on a centrifugal stage using a commercially available steady state 3D CFD algorithm is presented in the paper. The principal finding from this study is that for a typical product application, the steady state stage simulation is in good agreement with the available test data. In particular, the diffuser characteristics of loss and recovery predicted by the stage CFD analysis agree very well with the test data. The results indicate that for centrifugal compressors in this class, steady state stage CFD may be an effective design tool.

INTRODUCTION

The question has been raised a number of times if stage analysis is necessary to advance the state of the art in centrifugal compressors. Further, the complexity of that stage analysis in terms of amount of features included, steady versus unsteady, etc. that is needed has also been questioned.

An in house CFD code for impeller design had been in production at GE for quite some time and had proven itself to be very useful in optimizing impeller designs. GE started a centrifugal compressor CFD validation project in early 1999 with the goal of validating a CFD code for diffuser

design. Many investigators have numerically studied the aerodynamics of a centrifugal compressor stage [1] through [4]. Some had concluded that unsteady stage CFD was necessary for centrifugal stage predictions.

As part of the current study, GE investigated isolated and stage calculations. Although the results of the isolated impeller analysis confirmed that isolated CFD is suitable for impeller design, the results of the isolated diffuser effort was rather disappointing: the team concluded that using an isolated diffuser analysis, there was no way to rationally match the recovery to throat data for a series of diffuser designs. Individually the analysis for each design could be matched to the data by arbitrarily varying the inlet angle, but there was no systematic way to predict what this angle should be. The team concluded that a stage analysis was necessary.

A number of different approaches to centrifugal stage analysis were attempted. After much effort, the team has been successful in calculating the stage performance of a centrifugal compressor using a steady state approach. This paper summarizes the results of this study.

TECHNICAL APPROACH

* Copyright © 2002 by General Electric Company, Published by the International Council of the Aeronautical Sciences, with permission.

The Stage Geometry

The centrifugal stage selected for this study is a medium pressure ratio stage used as a component of the compression system of one of GE's commercial aircraft engines.

As depicted in Figure 1, the stage is composed of a high inlet radius ratio, impeller

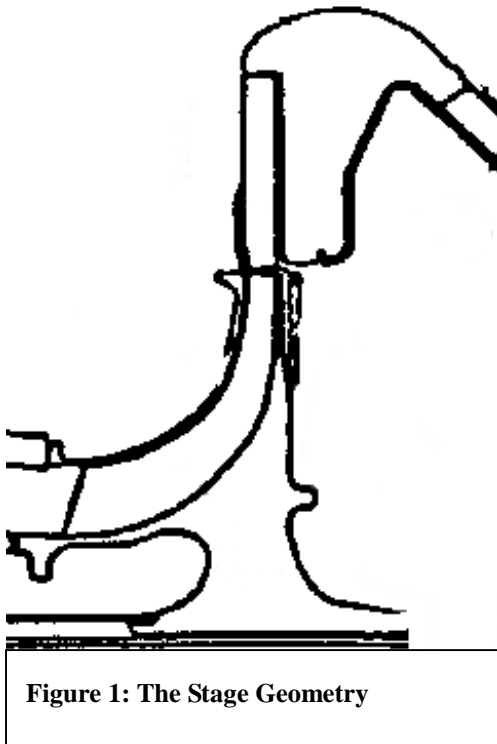


Figure 1: The Stage Geometry

matched with a passage-type diffuser (GE patented [5]). The diffuser discharges into an axi-symmetric bend equipped with de-swirling vanes at the downstream end.

The impeller has both full and splitter blades. The diffuser passages have a unique inlet configuration. The vane-less space is characterized by unsymmetrical vortex-generators, which are a forward continuation of the straight partial leading edge of the passage.

This stage was tested in GE Centrifugal Component Vehicle (CCV) at ambient inlet

conditions. The inlet conditions were obtained from a comprehensive transverse-traverse. The flow rate was measured by a calibrated Venturi. The total temperature and pressure at the stage exit were measured with three rakes with four 4 immersions each. The impeller tip static pressure was measured as the average of four static pressures 90° apart. Also, impeller tip forward and aft cooling bleeds were measured with separate orifice systems. The impeller total pressure is calculated from the above measurements assuming an impeller tip blockage of 0.9.

The Solution Algorithm

The computational analyses described in this paper have been performed with the CFX-TASCFLOW and CFX-5 codes developed by AEA Technology. Although these two codes have the same numerical scheme, CFX-TASCFLOW is a structured grid code while CFX-5 can handle both structured and unstructured grids. For the isolated impeller analysis, both the $k-\epsilon$ turbulence model with wall functions and the Shear Stress Transport (SST) model were used. For the isolated diffuser and stage analyses, the $k-\epsilon$ turbulence model with wall functions was used.

The solution of 3D, viscous turbulent, high speed compressible flows are performed in multiple reference frames. In a typical centrifugal application, the impeller blade rows are solved in a rotating frame of reference while the diffuser is solved in a stationary frame of reference. In a stage computation, the transfer of information between the rotating and stationary reference frame are handled through generalized specified interface attachments. These generalized interface attachments need not be node matched. This procedure allows independent development of grid for each component such as the impeller and the diffuser and then they can be patched together with an interface zone for a stage computation.

Component analysis for both the impeller and the diffuser were performed using both the structured

and unstructured grid strategy. The goal was to arrive at a consensus for choosing the optimal procedure for a design environment application.

CFD Analysis Methodology and Grid

For isolated impeller analysis, the exit of the impeller was somewhat extended to avoid the influence of the CFD exit boundary on the predicted results. An exit mass boundary condition was imposed on this CFD boundary corresponding to that derived from the test data. The inlet CFD boundary extended from the leading edge of the impeller blade where the span wise variation of the inlet total pressure, inlet total temperature and inlet flow angle derived from the test data were used as the boundary condition for the CFD solution. No slip and adiabatic wall conditions were used for all solid surfaces. Periodic boundary conditions were imposed upstream and downstream of the blade row.

In order to evaluate the architecture of the grid required, attempts were made to perform a steady impeller analysis using both structured and unstructured grid topology corresponding to a design point. A typical unstructured grid topology for the impeller included surface inflation (a structured layer of grid adjacent to any solid surface) and about 229,000 nodes while a typical topology for a structured grid included 160,000 nodes.

Diffuser grid topology provided a challenge due to its geometry shape from the exit of the impeller to the throat. The exit of the diffuser contained the 3-D bend, as shown in Figure 2, but not the de-swirling vane. For the isolated diffuser analysis an unstructured grid was employed. For the stage analysis, a structured grid generated in house was employed. This structured grid takes advantage of the block-off option available in TASCFLOW.

The exit boundary condition was typically either a mass flow or an exit static pressure condition depending on whether the CFD simulation is being performed on stall/ design side or choke side of the speedline. The inlet condition of the diffuser also presented a significant uncertainty in the isolated

diffuser CFD simulation. Other than a circumferentially averaged wall static pressure & a total outlet temperature at the diffuser exit, no other test data was available to derive an inlet profile at the diffuser inlet for the isolated diffuser CFD analysis. Pending a stage analysis, an impeller exit predicted profile of total pressure, total temperature and angle, modified to account for the test level of pressure and temperature as well as the bleed flow between the impeller and diffuser was used.

Stage analysis was performed using structured grid only. For stage analysis the component impeller and diffuser grids were patched up using a transition zone with appropriate definitions of the grid interfaces. Figure 2 shows a sketch of the test rig showing all components of the test rig: impeller, diffuser, bleed locations, diffuser bend and de-swirler.

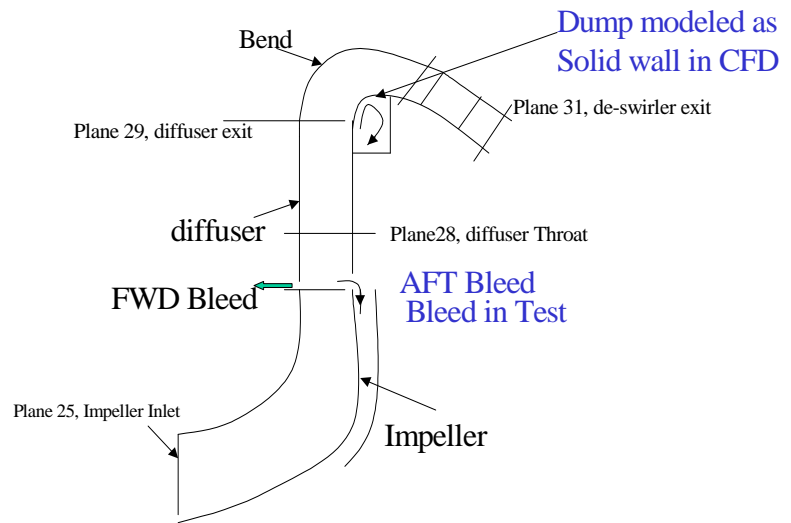


Figure 2: Stage CFD Model

For the CFD model the bleed has been modeled as normal to hub and casing planes. Also notice that there is a flow dump at the exit of the diffuser, which essentially results in a large recirculating volume. This volume was not modeled in the current CFD model. The face of this volume was modeled as a solid wall.

Figure 3 shows a typical grid utilized for the stage analysis using the mixing plane boundary condition approach at the impeller- diffuser interface. This grid consists of four blocks: impeller (68x43X21 streamwise, cross and spanwise), transition (4x28x26), diffuser (145x31x31) and 3D bend (40x18x18). To improve turn around time for CFD runs, the impeller grid size was reduced significantly.

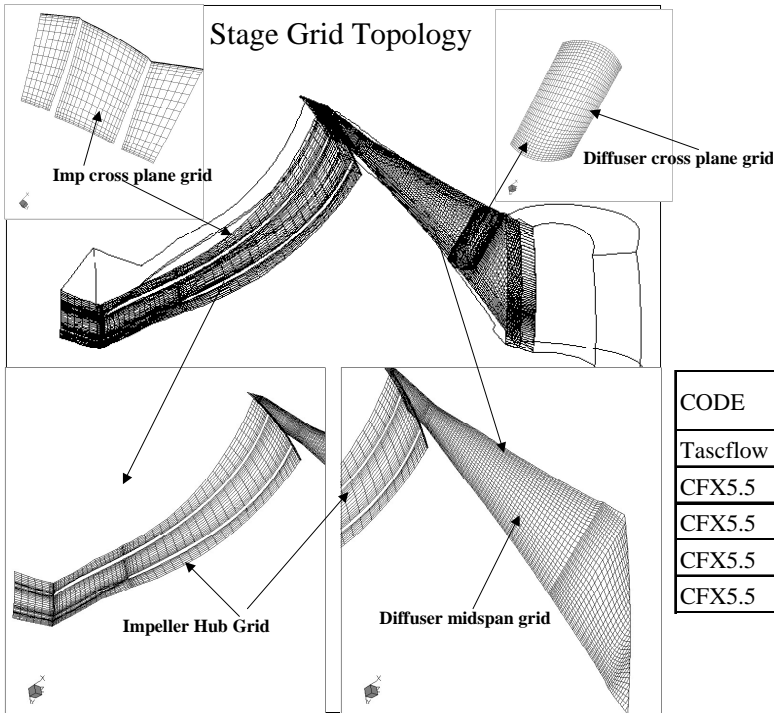


Figure 3: The Stage Grid

Roughly 48 stream wise nodes have been used from the impeller exit to the diffuser throat. The block-off option has been used to transition from the throat to the impeller exit. Note that the mixing plane interface boundary condition requires matching spanwise height at the interfaces. Averaging in the circumferential direction allows mismatched circumferential width. All other boundary conditions are similar to those adopted for impeller at the inlet and those used for the diffuser exit.

The detailed results obtained from this methodology will be described next.

RESULTS

Isolated Impeller Calculation Results

For the isolated impeller simulation, both a 229,000 node inflated unstructured grid and a 161,000 node structured grid were utilized. For both cases the grid was arrived at through an extensive grid refinement studies, the details of which are not presented here. A study of the k-ε model versus the SST model was also performed.

Table 1 shows a design point comparison of the CFD results with the test data.

TABLE 1: Isolated Impeller CFD Results

CODE	GRID	TURBULENCE MODEL	PR/PRtest	TR/TRtest	$\eta - \eta_{test}$ Points
Tascflow	161k, structured	$\kappa - \epsilon$	1.0098	1.0077	-1.44
CFX5.5	161k, structured	$\kappa - \epsilon$	1.0006	1.0043	-1.21
CFX5.5	229k, unstructured	$\kappa - \epsilon$	0.9755	0.9990	-1.92
CFX5.5	229k, unstructured	SST	0.9885	0.9999	-0.99
CFX5.5	161k, structured	SST	1.0795	1.0229	0.10

Since the measured centrifugal compressor exit temperature can be assumed to be the same as the impeller exit temperature, a match to temperature was considered more important (recall that the calculated test total pressure at the impeller exit includes a blockage assumption). The results from these studies were that the 161,000 node structured grid solution was very similar to the 229,000 node unstructured grid solution. The k-ε model, in addition to being more robust than the SST model, also yields a better match to the data in terms of total temperature ratio. For these reasons, the k-ε model with structured grid was chosen for the stage solution.

Figure 4 shows the comparison of the efficiency from the isolated impeller CFD with the test data from stage choke to stall at the design speed. Since the diffuser not the impeller sets the choke flow, and the impeller solution tends to over pressure, one would not expect a close match on the choke side. Results near peak efficiency are in better agreement with the test data.

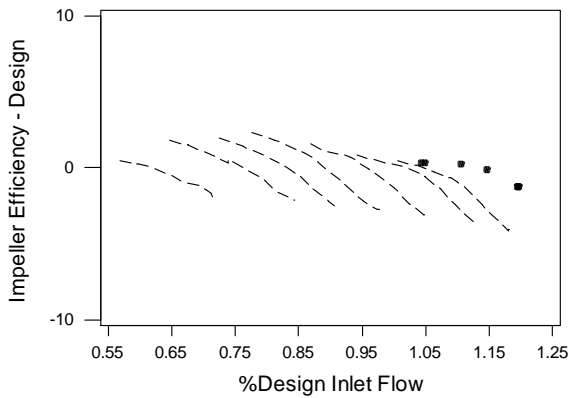


Figure 4: Isolated Impeller Results: Data is Dashed Line; CFD is Solid Symbol

Isolated Diffuser Calculation Results

Grid development for diffuser using unstructured topology required a major development effort that was first initiated with parametric development of a part file in UG from diffuser coordinates. After this effort was complete, unstructured grid from three different configurations were generated. A series of isolated analyses were run on three different geometries from choke to stall at three different speeds.

Figure 5 shows a comparison of the test data at the design point versus two different CFD runs on the same geometry. The difference between the two CFD runs is only in inlet angle. One can see that even though the static pressure aft of the throat is

very similar for both cases, the behavior forward of the throat is very different. When the inlet angle was perturbed arbitrarily by one degree, a better match to test data was obtained. A one degree increase in impeller exit angle implies a large increase in impeller temperature rise. Since there was no physical justification for the one degree difference, the team rejected this as a solution. In addition, when the same adjustment was applied to other geometries, it failed to improve the match to their associated data.

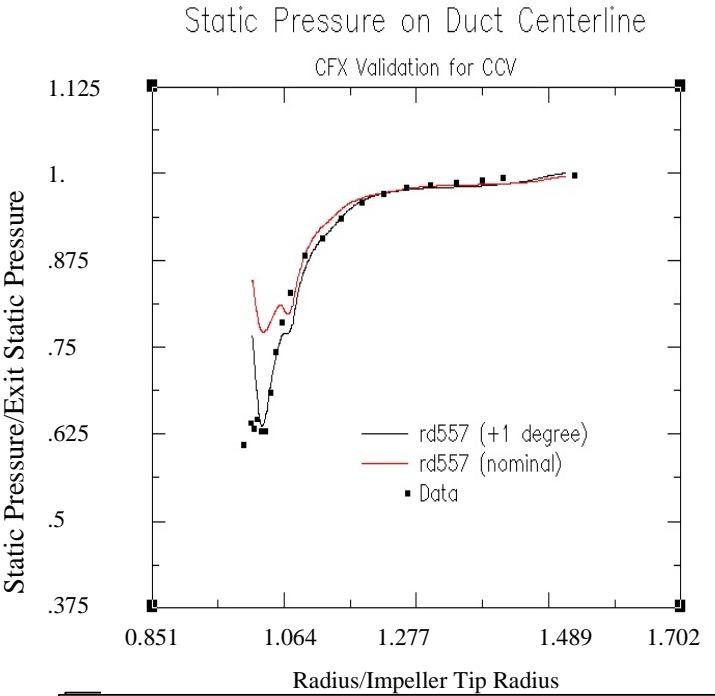


Figure 5: Isolated Diffuser Results

Steady Stage Calculation Results

Mixing plane stage analysis was performed for a speed line from choke to stall for the CFD model & the grid strategy described earlier. Figure 6

shows computed overall pressure recovery and the throat pressure recovery of the diffuser as compared to the test data. The results show very good agreement between the CFD simulation and the test data. The overall recovery is predicted very closely all along the throttle line, including the peak recovery level. More remarkable is the recovery to the throat comparison. Recovery to the throat, which is a very important design parameter, is very well predicted in this simulation. The choke flow is over predicted by about 2%. On the stall side, the simulation is close to the stall flow, although the simulation does run into numerical instabilities somewhat early.

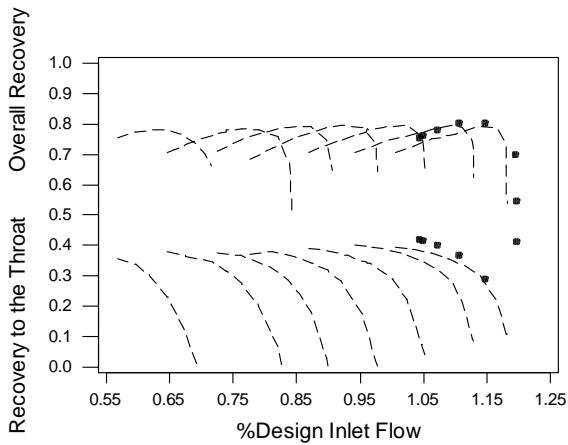


Figure 6: Overall Recovery and Recovery to the Throat

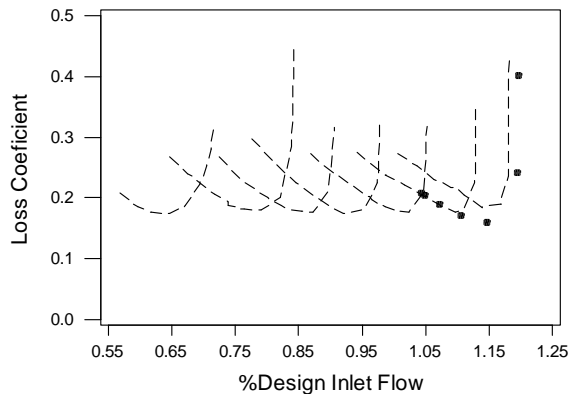


Figure 7: Diffuser Loss Coefficient; Data is Dashed Line; CFD is Solid Symbol

The calculated loss coefficient for both the test and CFD for this diffuser is shown in Figure 7. Again good agreement with test data is observed from choke to the stall. The CFD predictions for the choke side of the map seem to be somewhat over predicted. There are a number of potential reasons for this including the uncertainty in impeller radial growth and impeller/shroud clearance distribution that might not have been properly accounted for in this CFD model.

Figure 8 shows a comparison of the impeller efficiency from two different CFD runs: isolated impeller analysis and stage analysis. As can be seen from the figure, the results from the stage simulation are very similar to that from the isolated impeller solution.

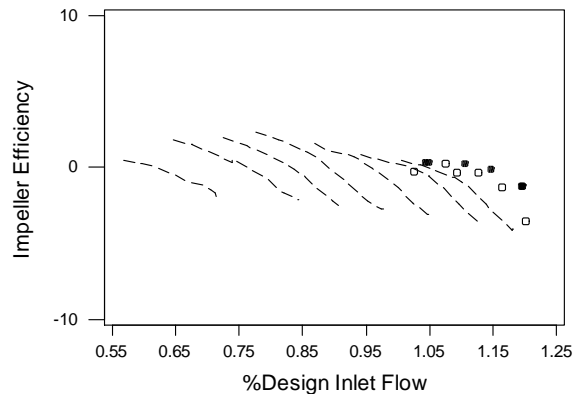


Figure 8: Impeller (Efficiency – Design Efficiency); Data in Dashed Line; Isolated CFD in Open Symbol; Stage CFD in Solid Symbol

Figure 9 shows the overall efficiency for this CFD simulation. Note that since the dump aft of the diffuser and the de-swirl vane are not included in this analysis, the expectation would be that the CFD

would over-predict efficiency by about two points. This explains the difference between the CFD solution and the test data. This inadequacy in the CFD model will be addressed in future efforts.

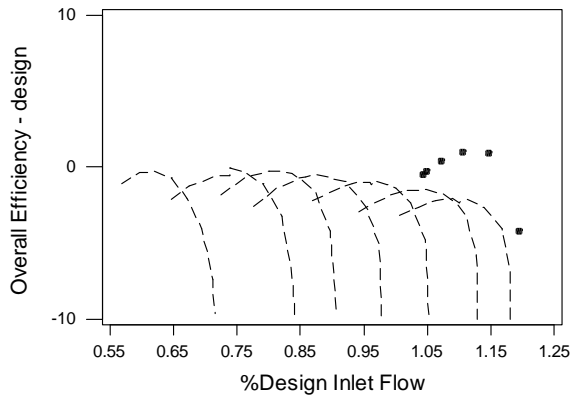


Figure 9: (Overall Efficiency - Design Overall Efficiency); Data is Dashed Line; CFD is Solid Symbol

Some details of the CFD simulation at 101% design mass flow are discussed next. Figure 10 shows the absolute Mach number contours at the mid span section of the centrifugal stage. Notice from this figure that the flow Mach number at inlet of the diffuser is near 0.9-0.95. Near the exit of the diffuser a fairly low Mach number fluid domain is observed. However, synthesis of CFD result does not show any reverse flow in this region. Notice a small low momentum fluid near the leading edge of the diffuser, however no reverse flow was found in this domain. From a design standpoint, this low momentum fluid domain at the inlet of the diffuser is an area of potential improvement.

Figure 11 shows a similar absolute Mach number plot in the cross-stream planes of the diffuser from inlet to the diffuser exit. Pockets of low momentum fluid flow patterns are clearly observed as one moves from the leading edge to the exit of the diffuser.

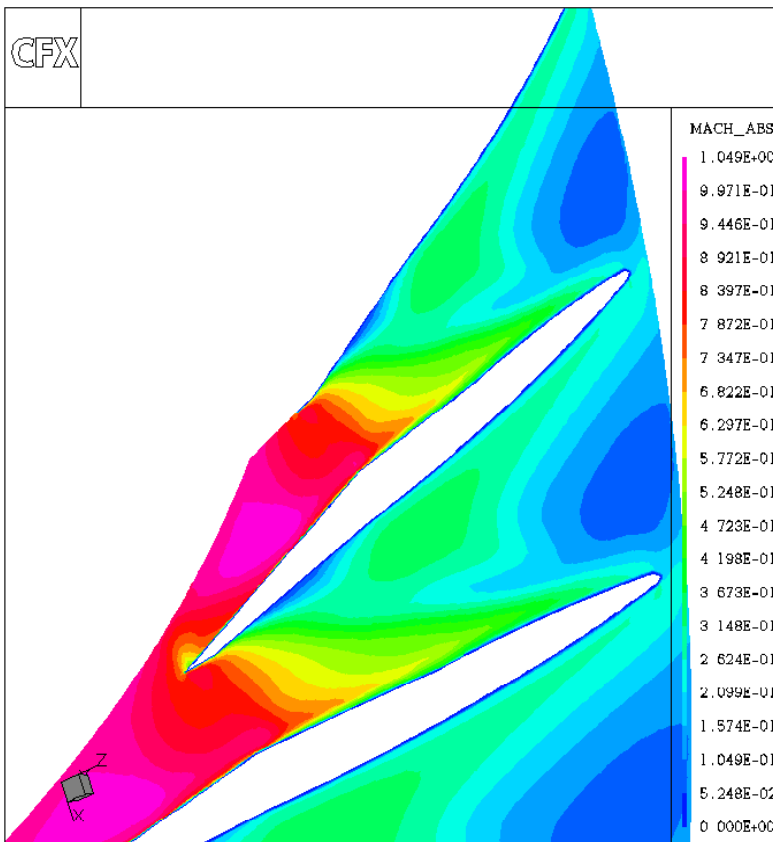


Figure 10: Absolute Mach# at Mid-Span Section

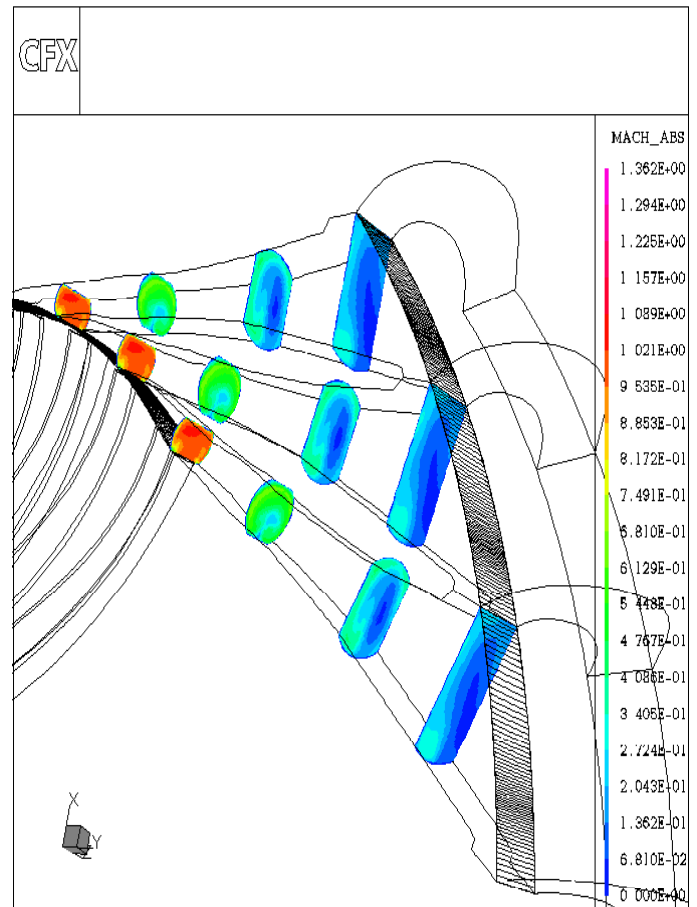


Figure 11: Absolute Mach# for a Series of Cross-Stream Planes

The secondary flow development can also be observed in the diffuser through Figure 12. This plot shows secondary flow at several stream wise sections in the diffuser. One can observe the intense flow mixing near the leading edge that subsides towards the exit of the diffuser. The CFD confirms the concept of the vortex generator to enhance mixing thereby reducing diffuser throat blockage. This reduction in diffuser throat blockage is well known to improve diffuser performance.

- Isolated impeller analysis is comparable to stage analysis for impeller design.
- Isolated diffuser analysis is unacceptable for diffuser design.
- Steady stage analysis, when performed carefully, is suitable for centrifugal compressor designs in this class.
- CFX offers the advantage of being able to handle both structured and unstructured grids.
- Although currently structured grid offers the radial compressor designer the advantages of easier control of the grid and shorter computing time, with development this advantage should be minimized.

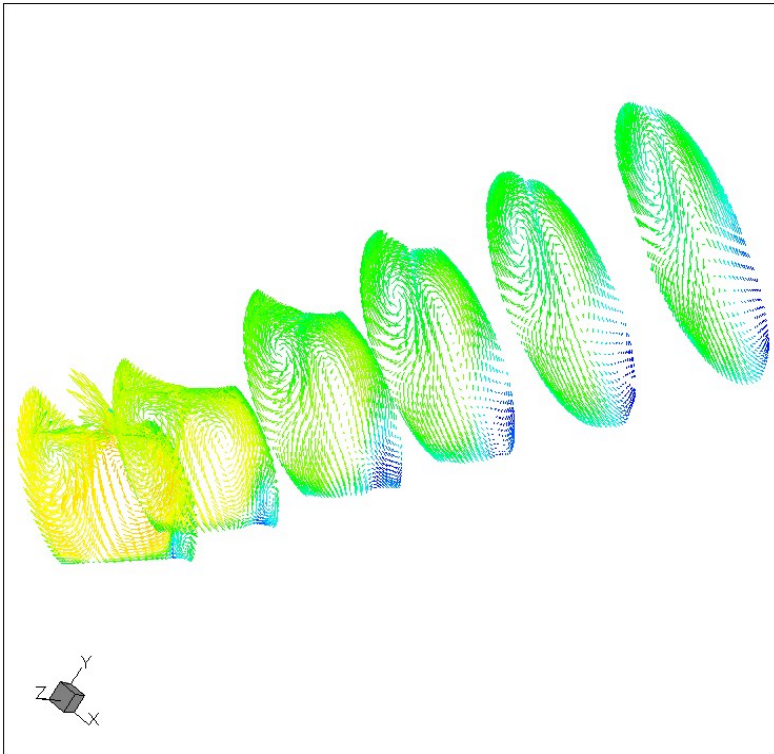


Figure 12: Secondary Flow Velocity Vectors

CONCLUSIONS

The conclusions from this study are as follows:

ACKNOWLEDGEMENTS

The authors would like to acknowledge the efforts of Caroline Granda at GEAE and Mark Braaten and Karen Zhang at GE Global Research Center for their assistance with the diffuser modeling, Rob Broberg, Mike Chudiak and Feng Shi at AEA Technology for their assistance with the stage analysis and Joseph Machnaim at EACOE for his assistance with the isolated impeller analysis. The authors would like to thank Aspi Wadia for permission to publish this paper.

REFERENCES

1. Dawes, W.N., 1995, "A Simulation of the Unsteady Interaction of a Centrifugal Impeller With Its Vaned Diffuser: Flow Analysis," ASME Journal of Turbomachinery, Vol. 117, pp. 213-222.
2. Domercq, O., and Thomas, R., 1997, "Unsteady Flow Investigation in a Transonic Centrifugal Compressor Stage," AIAA paper No. 97-2877.
3. Peeters, M., and Sleiman, M., "A Numerical Investigation of The Unsteady Flow in Centrifugal Stages," Proceedings of ASME TURBOEXPO 2000, May 8-11, Munich Germany, Paper No. 2000-GT-0426.
4. Shum, Y.K.P., Tan, C.S., and Cumpsty, N.A., "Impeller-Diffuser Interaction In Centrifugal Compressor," Proceedings of ASME TURBOEXPO 2000, May 8-11, Munich Germany, Paper No. 2000-GT-0428.

5. Bryans, A.C., 1986, "Diffuser For a Centrifugal Compressor," U.S. Patent No 4,576,550.